PROCEEDINGS OF SPIE

SPIEDigitalLibrary.org/conference-proceedings-of-spie

Single-photon generation through cavity-STIRAP in a neutral QD embedded in a micropillar cavity: an FDTD model study

Gaby Slavcheva, Mirella Koleva, Kai Müller, Robert Taylor

Gaby M. Slavcheva, Mirella V. Koleva, Kai Müller, Robert A. Taylor, "Single-photon generation through cavity-STIRAP in a neutral QD embedded in a micropillar cavity: an FDTD model study," Proc. SPIE 12243, Photonics for Quantum 2022, 122430E (19 July 2022); doi: 10.1117/12.2635200

SPIE.

Event: Photonics for Quantum, 2022, Rochester, NY, United States

Single-photon generation through cavity-STIRAP in a neutral QD embedded in a micropillar cavity: an FDTD model study

Gaby M. Slavcheva[a], Mirella V. Koleva[a], Kai Müller[b], and Robert A. Taylor[c]

[a]Quantopticon Ltd., 13 Broomfield, Guildford GU2 8LQ, United Kingdom
[b]Walter Schottky Institut and Physics Department, Technical University of Munich, Am Coulombwall 4, 85748 Garching, Germany
[c]Clarendon Laboratory, Department of Physics, University of Oxford, Oxford OX1 3PU, United Kingdom

ABSTRACT

We investigate cavity-assisted Stimulated Raman Adiabatic passage (STIRAP) schemes in semiconductor quantum dots (QDs) embedded in an optical cavity as a route for generation of high-quality single photons with programmable waveform. This work addresses the need for high-purity, indistinguishable photons in linear quantum computing, boson sampling, and quantum communications. We develop a time-dependent Maxwell-pseudospin model of single-photon generation through cavity-assisted adiabatic passage in a Λ-system isolated in a neutral InAs QD in a realistic GaAs/AlGaAs micropillar cavity. As a model Λ-system, we consider QD biexciton triplet states coupled to dark-exciton states by a circularly polarised pulse and a cavity field. Our simulations demonstrate control of the emitted single-photon pulse waveform by the driving pulse characteristics: shape, duration, intensity and detuning.

Keywords: cavity-QED, single photons, STIRAP, semiconductor quantum dots, micropillar cavities, Maxwell-pseudospin equations, Finite-Difference Time-Domain method

1. INTRODUCTION

Producing number-states of light is a challenging problem that is central to the practical use of non-classical states of light. Quantum information technologies require the development of a new type of light source in which the photon number can be carefully controlled. Solid-state quantum emitters, and in particular semiconductor quantum dots (QDs) have emerged as front runners in recent years[1] with a number of groups reporting near-unity quantum purity for dots embedded in optical cavities and overall efficiency at least 10 times the one of the heralded sources, *e.g.* based on spontaneous parametric down conversion in nonlinear crystals. However, self-assembled QDs inevitably vary in size and shape, hence the photons they emit are not identical. The spectral inhomogeneity of these emitters is a significant obstacle for construction of scalable quantum-photonic networks and more complex quantum devices. For instance, the use of QDs is prohibitive for protocols that involve interference of identical photons on photon-photon gates, such as linear optical quantum computing[2], or that involve the exchange of a photon between two qubits[3,4]. Strikingly, inhomogeneities of the QDs in terms of emission wavelength and rate can be overcome by using adiabatic passage techniques, such as cavity-assisted Stimulated Raman Adiabatic Passage (STIRAP) processes[5–8].

The possibility of single-photon generation through cavity-assisted adiabatic passage in a Λ-system with two ground states has been pointed out in the 90s. A systematic procedure for single-photon state generation using cavity-QED interaction, which forces the ground state of the cavity mode to evolve into an arbitrary quantum state at a predefined time, has been proposed in[9]. The basic principle has been theoretically demonstrated on a three-level Λ-system driven by two classical fields at two-photon resonance (common detuning), taking advantage of the SU(N) coherence vector picture[10]. This approach has been extended for one classical and one quantised field in[11–14] for atomic systems.

Send correspondence to G.M.S.: E-mail: gaby@quantopticon.co.uk, Telephone: +44 (0)7810 786255

Photonics for Quantum 2022, edited by Donald F. Figer, Proc. of SPIE Vol. 12243, 122430E

This paper investigates cavity-assisted Stimulated Raman Adiabatic Passage (STIRAP) schemes as a route for generation of high-purity and high-indistinguishability programmable single photons, using QDs embedded in high-Q micropillar cavities. In cavity-STIRAP, under the two-photon resonance condition (common detuning of the driving pulse and the cavity coupling field), an adiabatic state transfer takes place in which a Raman photon is emitted into the resonator mode[15]. This process is unique as the pulse shape of the emitted photon is determined by the driving field, which allows for the generation of single photons with customisable pulse shape[16]. Most importantly, cavity-STIRAP enables generation of indistinguishable photons from an ensemble of non-identical QDs, as the driving pulses may have common detuning from the excited level. The frequency of the emitted light is determined only by the excitation laser frequency and the cavity frequency, and not by the emission energy of the QDs. Moreover, since the pulse shape is determined by the QD-resonator system parameters, QDs with different emission rates (lifetimes) can be used to generate identical photons by adjusting the driving strength.

We study a promising adiabatic passage scheme applied to a three-level Λ-system isolated in a neutral QD exciton embedded in a micropillar cavity, operating in the strong-coupling regime. By computing the quantum dynamics of the optical pulse interactions with the excitonic optical transitions we demonstrate control of the time evolution of the cavity-dot quantum system and identify adiabatic conditions for steering it towards a desired single-photon quantum state of the cavity field. We explore numerically the possibility of generating programmable single photons by identifying key parameters for control of the spectral and spatiotemporal properties of the single-photon wave packet. In addition, by running simulations on a variety of cavity geometries, we could identify optimised structure geometries yielding reproducible results for the generated single photons.

2. THEORETICAL MODEL

2.1 Cavity-assisted STIRAP scheme for single-photon generation with QDs

In the simplest implementation of the STIRAP scheme (Fig. 1), the pump and the Stokes fields couple the ground levels to the excited level. Both fields are detuned from the excited level generally with different detunings. The fields act in a counter-intuitive sequence: the system first interacts with the Stokes field, and subsequently with the pump laser. The Stokes laser (S) couples two empty states (which does not change the populations of the levels, ρ_{11}) and creates a coherent superposition of $|2\rangle$ and $|3\rangle$. Subsequently, the pump (P) couples the two empty states to $|1\rangle$, and under the two-photon resonance condition – namely, common detuning: $\Delta = \Delta_P = \Delta_S$ of the two fields from the excited state, a 'population trapped state' or 'dark state' is formed, which means that no population has been transferred to the excited state and the population is directly channelled to the final state, $|3\rangle$. A condition of the adiabatic transfer is $\Omega_P \gg \Omega_S$.

In the case of one classical field (*i.e.* the driving pulse) and one quantised field (the cavity mode), the Hamiltonian, as shown in[12], couples only states within the manifold: $|g_1, n\rangle$, $|e, n\rangle$ and $|g_2, n+1\rangle$, where $|n\rangle$ is an n-photon Fock state of the cavity mode (see Fig. 2a). In the dressed-state picture[17,18], the adiabatic energy eigenvalues consist of equidistant levels, $E_n = n\hbar\omega$, and the Autler-Townes doublets (superposition states), $E_n^{\pm}$ (see Fig. 2b). Interestingly, the eigenstate corresponding to $E_n = n\hbar\omega$ does not contain any contribution from the excited state (hence the term 'dark state') and is independent of the detuning. The possibility of adiabatic passage arises from its limiting behaviour: for a pulse sequence in which the driving field $\Omega(t)$ is time-delayed with respect to the cavity field, $g(t)$, the initial n-photon state, $|g_1, n\rangle$, may be adiabatically transformed into a final $(n+1)$-photon state, $|g_2, n+1\rangle$, hence the possibility of generation of Fock states of the cavity mode. As a special case, single-photon states are produced out of the vacuum (zero-photon) state.

Our goal is to develop a description of the adiabatic passage beyond the Rotating-Wave Approximation (RWA). RWA is a valid approximation only when: (i) a significant fraction of the pulse spectral bandwidth is near-resonant with the optical transition; (ii) the driving field is relatively weak, so that the Rabi frequency is small compared to the resonant transition frequency.

The strong driving regime is reached when the Rabi frequency approaches the resonant transition frequency. Under such conditions, complex dynamics can occur, such as fast beatings, and the resonant transition frequency can become a function of the driving field amplitude (Bloch-Siegert shift). Both effects arise from the counter-rotating terms that are present in a harmonic, oscillatory driving field, which are nevertheless ignored in the RWA.

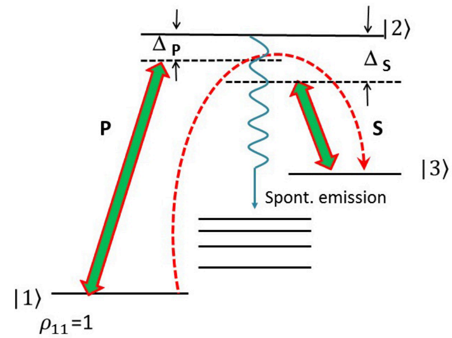

Figure 1. STIRAP scheme in a three-level Λ-system. The pump field, P, with Rabi frequency, Ω_P, is detuned from the excited level, $|2\rangle$, by detuning Δ_p. The Stokes laser field, S, with Rabi freqency Ω_S, is detuned from the excited state by detuning, Δ_S. The population is initially residing in the ground level, $\rho_{11} = 1$.

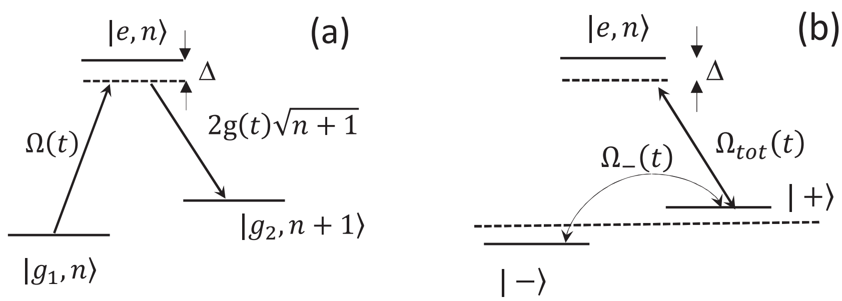

Figure 2. Three-level Λ-system in an optical cavity at two-photon Raman resonance. (a) Bare-state picture. The ground levels are denoted by $|g_1\rangle$ and $|g_2\rangle$, the excited state is denoted by $|e\rangle$. $|n\rangle$ represents an n-photon Fock state of the cavity mode and the states represent manifolds. $\Omega(t)$ is the Rabi frequency of the driving classical laser field, $g(t)$ is generally time-dependent coupling of the QD transition to the cavity mode with frequency ω, Δ is the common detuning of the laser and the cavity mode. (b) Dressed-state picture. The states denoted by $|+\rangle$ and $|-\rangle$ correspond to the doublet states, $E_n^{\pm}$. One effective field, with Rabi frequency $\Omega_{tot}(t) = \sqrt{|\Omega(t)|^2 + |g(t)|^2}$, couples the excited level to the bright state, $|+\rangle$; another effective field, with Rabi frequency $\Omega_- = \frac{\dot{\Omega}g - \dot{g}\Omega}{\Omega^2}$, couples non-adiabatically the two superposition states, $|+\rangle$ and $|-\rangle$.

Although the picosecond pulse excitations that we are going to simulate are not broadband high-intensity pulses, and therefore do not violate condition (ii), an approach beyond the RWA is needed, since the STIRAP excitation requires relatively large detuning of the excitation pulse from the excited state. The excitation is therefore off-resonant and so clearly violates condition (i). On the other hand, we will model different pulse shapes in order to demonstrate imprinting the driving pulse characteristics onto the generated single-photon pulse waveform. Therefore, the significant spectral components of the driving field may be displaced relatively far from the resonance, thereby violating the resonance condition. In addition, we study spatially dependent quantum interference effects in realistic extended quantum-optical devices that might be strongly influenced by complex spatiotemporal dynamics that are usually obscured by the RWA approximation.

As a model Λ-system, we consider QD biexciton triplet states coupled to dark-exciton states by a circularly polarised trigger pulse and a circularly polarised cavity field[19, 20] (Fig. 3); however the results apply generally to an arbitrary Λ-system in a QD.

We propose the design of a 25.5/25 DBR-pair GaAs/AlGaAs micropillar Λ-cavity (GaAs) of length $\lambda_{cavity} =$ 970 nm, with a neutral InGaAs QD embedded in the cavity centre. The target QD density is 1–10 μm^{-2} (10^8–10^9 cm^{-2}). The cavity is designed at a wavelength resonant with the transition between the excited biexciton

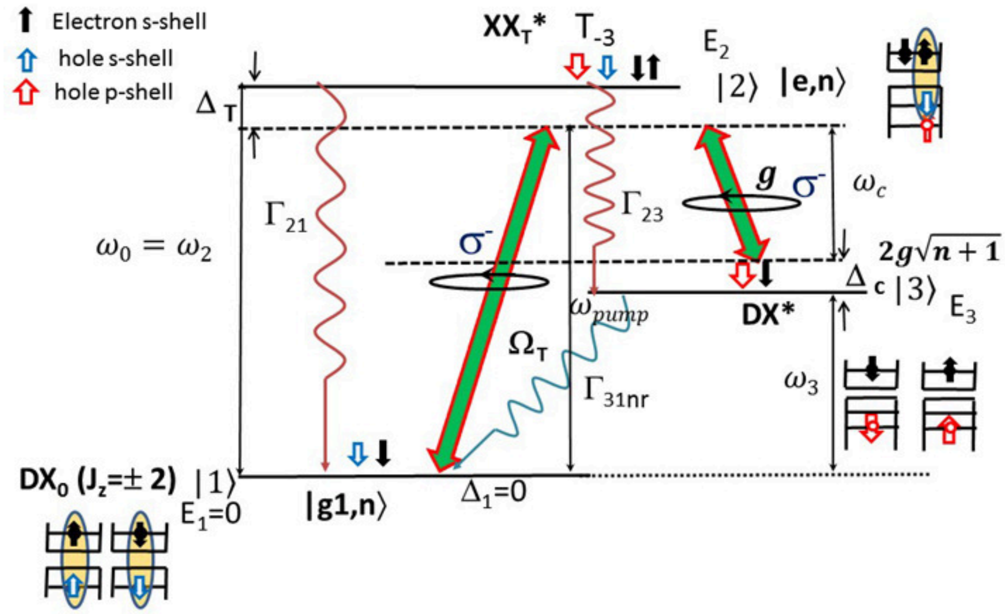

Figure 3. Cavity-assisted STIRAP scheme for single-photon generation in a neutral QD embedded in an optical cavity. Before the trigger pulse is applied ($\Omega_T = 0$) the dot is coupled to the cavity mode with dot-cavity coupling $g > 0$, g=const. The cavity is designed to be resonant with the optical transition between states $|2\rangle$: excited triplet state T_{-3} and $|3\rangle$: excited dark-exciton state DX^*. The cavity mode is left-circularly polarised (σ^-) and is detuned from the excited level by detuning, Δ_T and from the second ground state,$|3\rangle$, by Δ_c. The driving pulse is left-circularly polarised couples the dark-exciton state, DX_0 with $J_z = -2$ and the triplet state T_{-3} with detuning, Δ_T; Γ_{21}, Γ_{23} are spontaneous emission rates between the excited and the two ground levels, respectively. Γ_{31nr} is the non-radiative decay rate from the excited dark exciton level, DX^* to the ground dark exciton level, DX_0. ω_2 and ω_3 are the angular frequencies corresponding to the energy levels $|2\rangle$ and $|3\rangle$, respectively. The spin configurations of all three levels are displayed next to the corresponding energy levels.

triplet state, T_{-3} (with total spin projection $J_z = -3$), and the excited dark-exciton state, DX^* (with total spin projection $J_z = -2$), in a neutral QD[19–21], and the cavity mode is circularly polarised. Before the trigger pulse, T, is applied ($\Omega_T = 0$), the dot is coupled to a left-circularly polarised cavity mode with coupling strength, g, which implies a relationship for the mixing angle, θ[5]: $\tan(\theta) = \frac{\Omega_T}{2g} = 0$. Since the adiabatic dark-state eigenvector is given by $|\Psi_0\rangle = cos(\theta)|1\rangle - sin(\theta)|3\rangle$, preparing the system in state $|1\rangle$ is equivalent to preparing the whole system in the 'dark state', Ψ_0. The two-photon resonance condition is satisfied when $\Delta_T = \Delta_c = \Delta$, where Δ_c is the detuning of the cavity field from the final dark-exciton state. Under the two-photon resonance, and provided that the adiabaticity conditions are satisfied, the population is adiabatically transferred from $|1\rangle$ to $|3\rangle$. The transient photon emission rate is proportional to the population of level $|3\rangle$ and is also proportional to $\kappa\rho_{33}$[13], where κ is the cavity loss rate.

2.2 System Hamiltonian and master Maxwell's curl-pseudospin equations for a three-level system

In order to model the quantum dynamics of the optical excitation and single-photon generation through cavity-assisted adiabatic passage in a Λ-system, we deploy our time-dependent Maxwell-pseudospin model[22–24].

The system Hamiltonian, corresponding to Fig. 3, is given by:

$$\hat{H} = \hbar \begin{pmatrix} 0 & -\frac{1}{2}(\Omega_x - i\Omega_y) & 0 \\ -\frac{1}{2}(\Omega_x + i\Omega_y) & \omega_2 & -\frac{1}{2}(g_x - ig_y) \\ 0 & -\frac{1}{2}(g_x + ig_y) & \omega_3 \end{pmatrix}, \quad (1)$$

where $E_2 = \hbar\omega_2$ and $E_3 = \hbar\omega_3$ are the energies of state $|2\rangle$ and $|3\rangle$, and we have defined the Rabi frequencies, $\Omega_x = \frac{\mu}{\hbar} E_x$ and $\Omega_y = \frac{\mu}{\hbar} E_y$, with $\hat{\mu} = \langle i\, |e\mathbf{r}|\, j\rangle$ being the optical dipole moment matrix element between levels $|i\rangle$ and $|j\rangle$ (assumed a scalar) and complex cavity couplings, $(g_x - ig_y)$ and $(g_x + ig_y)$, where g_x and g_y are the couplings corresponding to the x- and y- electric-field components.

We derive master pseudospin equations for a three-level system using the generators of SU(3) Lie algebra and the Hamiltonian from Eq. 1, including the cavity coupling. The evolution of the 8-dimensional real coherence vector under the optical pulse excitations can be written as:

$$\frac{d\mathbf{S}}{dt} = \mathbf{MS} - diag\left(\frac{1}{T_1}, ..., \frac{1}{T_8}\right)\mathbf{S} \tag{2}$$

$$\hat{M} = \begin{pmatrix} 0 & g_y & 0 & 2\Delta & -g_x & 0 & \Omega_y & 0 \\ -g_y & 0 & \Omega_y/2 & -g_x & 0 & \Omega_x/2 & 0 & 0 \\ 0 & -\Omega_y/2 & 0 & 0 & 0 & -2\Delta & -g_y & \sqrt{3}g_y \\ -2\Delta & g_x & 0 & 0 & g_y & 0 & -\Omega_x & 0 \\ g_x & 0 & -\Omega_x/2 & -g_y & 0 & \Omega_y/2 & 0 & 0 \\ 0 & -\Omega_x/2 & 2\Delta & 0 & -\Omega_y/2 & 0 & g_x & -\sqrt{3}g_x \\ -\Omega_y & 0 & g_y & \Omega_x & 0 & -g_x & 0 & 0 \\ 0 & 0 & -\sqrt{3}g_y & 0 & 0 & \sqrt{3}g_x & 0 & 0 \end{pmatrix}, \tag{3}$$

where we have defined non-uniform relaxation times, T_i, $i = 1, 2, ..., 8$ of the pseudospin vector components to their equilibrium values. The first six of those are polarisation relaxation or dephasing times, and therefore the equilibrium value of the corresponding S-vector components are zero, while T_7 and T_8 have the physical meaning of spontaneous emission times describing the relaxation of the population components S_7 and S_8 to their equilibrium values, S_{7e} and S_{8e}, respectively.

We solve Maxwell's curl equations for a circularly polarised trigger pulse with Rabi ferquency, Ω_T, detuned from the excited level by a common detuning, Δ (Fig. 3):

$$\begin{aligned} \frac{\partial H_x(z,t)}{\partial t} &= \frac{1}{\mu}\frac{\partial E_y(z,t)}{\partial z} \\ \frac{\partial H_y(z,t)}{\partial t} &= -\frac{1}{\mu}\frac{\partial E_x(z,t)}{\partial z} \\ \frac{\partial E_x(z,t)}{\partial t} &= -\frac{1}{\varepsilon}\frac{\partial H_y(z,t)}{\partial z} - \frac{1}{\varepsilon}\frac{\partial P_x(z,t)}{\partial t} \\ \frac{\partial E_y(z,t)}{\partial t} &= \frac{1}{\varepsilon}\frac{\partial H_x(z,t)}{\partial z} - \frac{1}{\varepsilon}\frac{\partial P_y(z,t)}{\partial t}, \end{aligned} \tag{4}$$

where P_x and P_y are the macroscopic medium polarisations induced by the E_x and E_y components of the circularly polarised electric field.

Following our theoretical framework[23], we derive additional relationships between the polarisation components and the real pseudospin vector components:

$$\begin{aligned} P_x &= -\mu N_d S_1 \\ P_y &= -\mu N_d S_4, \end{aligned} \tag{5}$$

where N_d is the resonant dipole density.

We implement the 25.5/25 GaAs/AlGaAs DBR micropillar cavity through the refractive-index spatial profile. Perfectly transmitting boundary conditions are imposed at both the input and output device facets. The latter allows us to compute the cavity loss and Q-factor, which is usually assumed as an external parameter in the models. The pulse is launched from the right boundary of the simulation domain assuming a realistic experimental excitation through an optical fibre coupled to the top of the micropillar.

We self-consistently solve Eq. 4, Eq. 2, and Eq. 5 directly in the time domain, employing the FDTD time-stepping algorithm. The initial driving pulse is a circularly polarised Gaussian pulse with carrier angular frequency, ω_{det}, and central wavelength corresponding to the detuned $|1\rangle \rightarrow |2\rangle$ transition ($\lambda_{det} = 972$ nm, for detuning $\Delta = 0.5$ meV) and pulse duration, $T_p = \text{FWHM} = 50$ ps ($T_p = t_d\sqrt{4\ln 2}$):

$$\sigma^{\pm}\begin{cases} E_x\left(z=L,t\right) = \quad E_0 exp\left[-\left(t-t_0\right)^2/t_d^2\right]\cos(\omega_{det}t) \\ E_y\left(z=L,t\right) = \pm E_0 exp\left[-\left(t-t_0\right)^2/t_d^2\right]\sin(\omega_{det}t) \end{cases}, \tag{6}$$

where $\pm$ stands for right- $(+)$ or left- $(-)$ circularly polarised excitation.

In the weak excitation regime, the initial pulse amplitude, E_0, is determined from the condition for the pulse Rabi frequency, $\Omega_T = \mu E_0/\hbar = 2g$. In the strong excitation regime, it is chosen to be $100 \times 2g$.

2.3 Adiabaticity conditions

The term 'adiabatic' means that the rate of varying the control parameters is sufficiently slow so that a quasi-steady state is maintained all along the process. This rate must be reasonably larger than the material relaxation rates if the process is to be practical. Condition for adiabatic transfer can be derived by inspecting the adiabatic dark state, $|\Psi_0\rangle = cos\left(\theta\right)|1\rangle - sin\left(\theta\right)|3\rangle$. For $\Omega_T \gg 2g$, $\tan\left(\theta\right) = \frac{\Omega_T}{2g} \gg 1$, leading to $\theta \rightarrow \frac{\pi}{2}$ that implies evolution from $|1\rangle$ to $|3\rangle$. On the other hand, in order to assure adiabatic following, the slope of the trigger pulse has to be sufficiently small to satisfy the adiabatic constraint $\left|\dot{\theta}\right| \ll |\omega_0 - \omega_{\pm}|$, where ω_0 is the dark-state eigenfrequency and $\omega_{\pm}$ are the doublet eigenfrequencies. This condition results from the requirement that the probability for transitions from the dark to other states be negligible, *i.e.* the dark state is energetically well separated from the doublet states throughout the interaction and that the non-adiabatic transfer between these states is not significant. Assuming a Gaussian pulse with pulse duration (FWHM) T_p, and peak intensities of Ω_{max} and g_{max}, the necessary condition for adiabatic following[12,13] is:

$$\Omega_{\max}T_p,\ 2g_{\max}\sqrt{n+1} \gg 1, \tag{7}$$

where $n = 1$ for single-photon generation, whereby the single-photon state is produced from adiabatic passage out of the vacuum. The above relation means that the trigger pulse cannot be shorter than g^{-1}.

As the ideal adiabatic transfer should occur when the passage involves a single manifold (labelled by $|n\rangle$), transitions between a given manifold and different $|n\rangle$ manifolds would lead to a degradation of the process. Such undesirable couplings could, for instance, arise from cavity damping and spontaneous emission, and therefore the technique will be optimised when:

$$\Omega_{\max}, g_{\max} \gg \Gamma, \kappa, \quad T_p \ll \kappa^{-1}. \tag{8}$$

3. NUMERICAL MODELLING

We perform simulations on a 25.5/25 DBR-pair GaAs/AlGaAs micropillar Λ-cavity (GaAs) with a neutral InAs QD described by a three-level Λ-system embedded in the centre of the cavity, where the latter is designed at $\lambda = 970$ nm. The trigger-pulse excitation is a Gaussian pulse with duration $T_p = 50$ ps and central wavelength $\lambda_{det} = 972$ nm that is detuned from $E_2 = \hbar\omega_2$ by $\Delta = 0.5$ meV[15]. The pulse intensity is varied through the initial pulse amplitude, E_0, that is chosen to satisfy $\Omega_T = 2g$, leading to $E_0 = 4.86343 \times 10^5$ Vm^{-1} for weak excitations (weak adiabaticity condition) and $\Omega_T = 100 \times 2g$, implying $E_0 = 4.86343 \times 10^7$ Vm^{-1}, for strong excitations (strongly satisfied adiabaticity condition).

The energies of the respective levels are calculated from the emission wavelengths and the spontaneous emission times given in the supplementary material of [20]: $\lambda_{12} = 959$ nm, $\lambda_{23} = 970$ nm. The exciton recombination energy is $E_X = 1.2834$ eV, the biexciton triplet-state energy is $E_{XXT} = 1.2771$ eV, the ground dark-exciton energy is evaluated at $E_{DX_0} = 1.283$ eV, and the excited dark exciton energy is computed to be $E_{DX^*} = 1.30525$ eV.

The cavity coupling is calculated from the oscillator strength of the resonant $|2\rangle \rightarrow |3\rangle$ transition:

$$f = \frac{2\hbar^2}{m_0 \left(E_X + E_{XXT} - E_{DX^*}\right)} \frac{m_0 E_p}{2\hbar^2}\,, \tag{9}$$

where $E_p = 22.71$ eV is the Kane matrix element for GaAs.

The mode volume is taken as the typical mode volume of a micropillar: $V_{mode} = 5(\lambda_{23}/n_{GaAs})^3$, where n_{GaAs} is the refractive index of GaAs. Then the cavity coupling strength is calculated from:

$$\mathrm{g} = \sqrt{\frac{\pi e^2 f}{4\,\pi\,\varepsilon_0\,\varepsilon_\mathrm{r}\,m_0\,\mathrm{V}_\mathrm{mode}}}\,, \tag{10}$$

leading to a value for the modulus of the coupling of $g = 1 \times 10^{11}$ s^{-1}. We will use the value of $g_x = g_y = 6.105 \times 10^{10}$ s^{-1}.

By varying the pulse parameters – *e.g.* pulse shape, duration, intensity, detuning – we identify parameters satisfying the adiabaticity conditions[13,25]. The simulation of the time evolution of the electric field components and level populations at the location of the QD are shown at the time $t = 450$ ps in Fig. 4. Our simulations show a slow adiabatic build-up of the final-state $|3\rangle$ population. The maximum population transferred during adiabatic passage is $\rho_{33} \approx 1.7 \times 10^{-4}$. Although the adiabatic condition $\Omega_T T_p \approx 6 \gg 1$, the adiabatic condition $\Omega_T \gg 2g$ is not satisfied, leading to a small fraction of the population being transferred to the final state.

In the strong excitation regime, we select $\Omega_T = 100 \times 2g$, so that the adiabaticity conditions $\Omega_T \gg 2g$ and $\Omega_T T_p \gg 1$ are strongly satisfied. The time evolution of the electric-field components, level populations, and the cavity emission are displayed in Fig. 5. Our simulations demonstrate Rabi oscillations of the population at high excitation pulse intensities, resulting in reshaping of the envelope of the cavity emission field in time. This implies that the single-photon pulse waveform can be controlled by the shape, duration, detuning and intensity of the driving pulse.

4. CONCLUSION

We developed and implemented a model of cavity-assisted STIRAP in a three-level Λ-system driven by a circularly polarised Gaussian pulse trigger and a cavity field, and applied it to the excited biexciton-dark exciton cascade in a neutral QD. We ran simulations in the low- and high-excitation regime and demonstrated adiabatic population transfer to the final state in both cases through the computed time evolution of the populations in the three-level system. The adiabatic transfer was more significant for higher trigger-pulse intensities where Rabi oscillations start to appear and the adiabaticity condition is strongly satisfied. We show reshaping of the cavity emission in time which depends on the driving-pulse characteristics. This is a step towards demonstrating programmable single-photon waveforms through optimising the driving pulse characteristics.

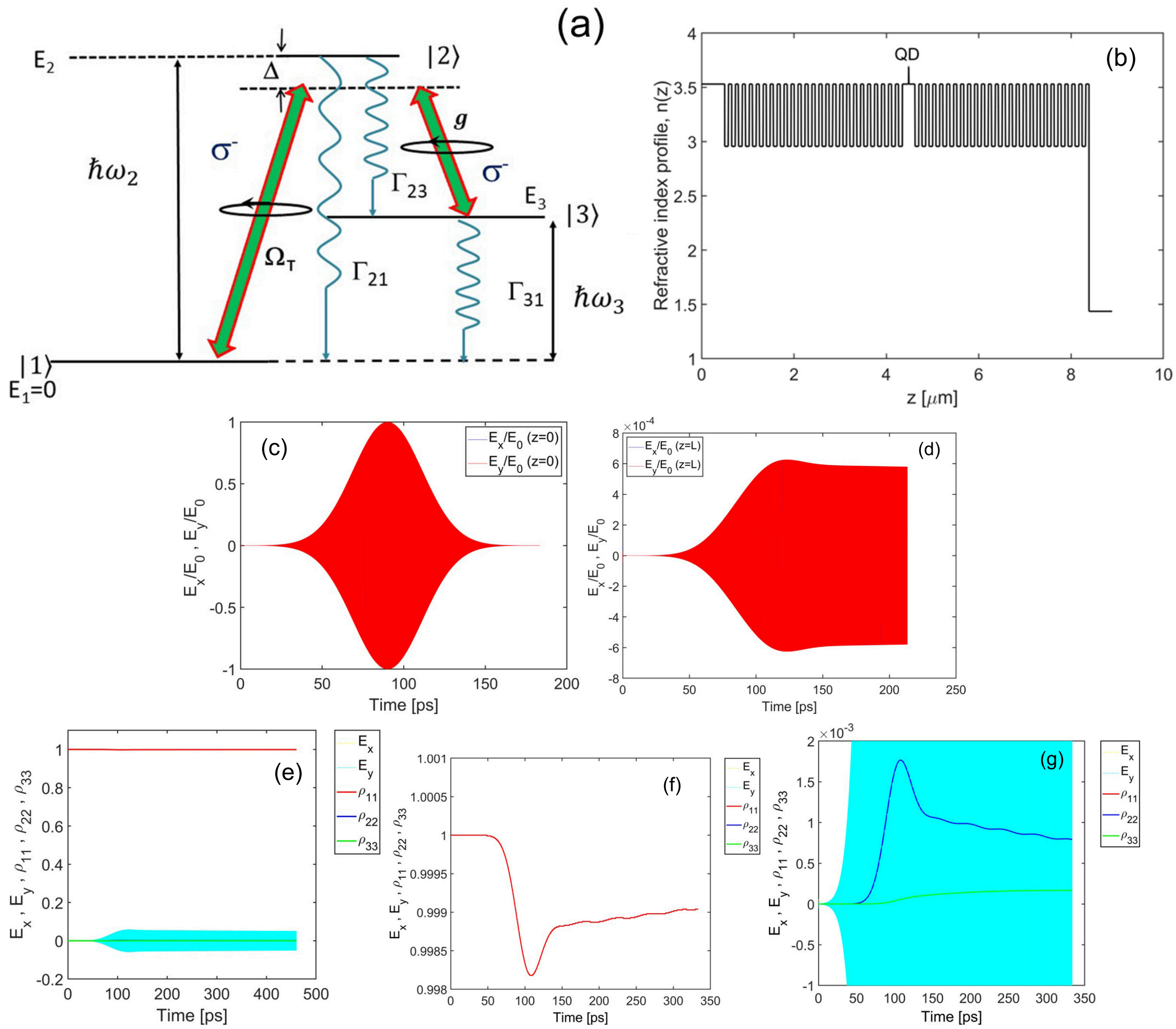

Figure 4. Simulations of (a) a three-level Λ-system driven by a Gaussian trigger pulse detuned by 0.5 meV from the excited-state energy, $E_2 = \hbar\omega_2$, with Rabi frequency $\Omega_T = 2g$, where the cavity coupling is $g = 6.105 \times 10^{10}$ s^{-1}. $\Gamma_{12} = 5 \times 10^8$ s^{-1} and $\Gamma_{23} = 3.0303 \times 10^9$ s^{-1} are spontaneous emission rates; $\Gamma_{31} = 1.42857 \times 10^{10}$ s^{-1} is the non-radiative decay rate. (b) Refractive-index profile of a QD-micropillar structure. Λ–cavity micropillar with cavity length $L_c = \lambda_{cavity}/n_{GaAs}$, designed at $\lambda_{cavity} = 970$ nm and consisting of 25.5/25 GaAs/AlGaAs bottom/top DBR pairs, containing a single InAs QD situated in the cavity centre. (c) Initial Gaussian pump pulse with Rabi frequency $\Omega_T = 2g$, pulse duration T_p = FWHM = 50 ps, at $\lambda_{det} = 972$ nm: detuned wavelength injected from the rightmost facet of the micropillar structure. The initial pulse amplitude is $E_0 = 4.86343 \times 10^5$ Vm^{-1}, which was calculated from $\Omega_T = 2g$. (d) Time evolution of the cavity emission out of the leftmost facet of the micropillar structure. (e) Time dynamics of the electric field and level populations at the location of the QD at $t = 450$ ps. (f) Time dynamics of the ground-state population, ρ_{11}, at $t = 333.5$ ps. (g) Time evolution of the populations ρ_{22} and ρ_{33} of levels $|2\rangle$ and $|3\rangle$, correspondingly, showing adiabatic build-up of the final-state population (green curve), $\rho_{33} \approx 1.7 \times 10^{-4}$.

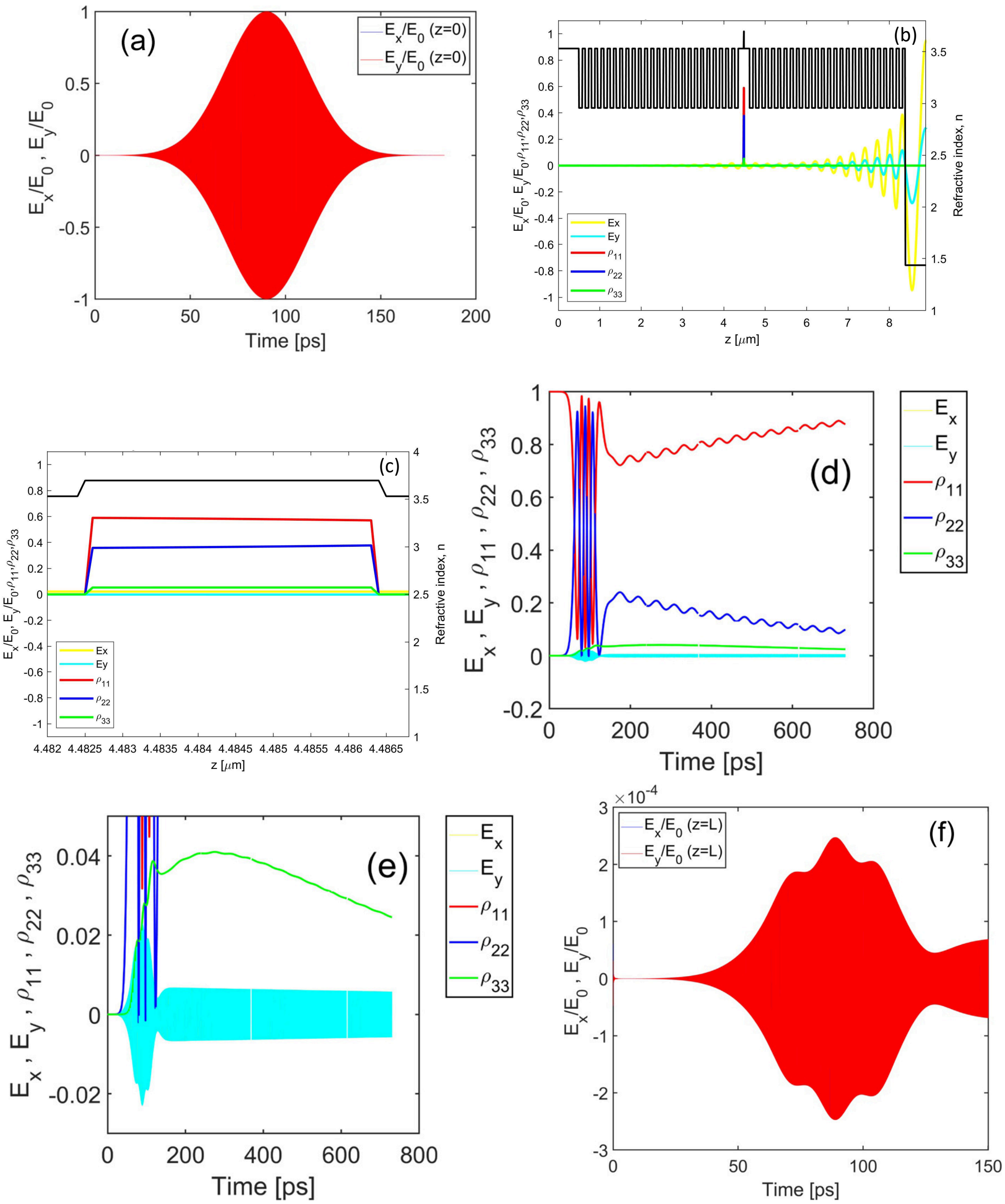

Figure 5. Simulations of a three-level Λ-system (Fig. 4a) driven by (a) Gaussian pulse with Rabi frequency $\Omega_T = 100 \times 2g$ (pulse duration, $T_p = 50$ ps at $\lambda_{det} = 972$ nm) and the cavity coupling is $g = 6.105 \times 10^{10}$ s^{-1}, detuned by 0.5 meV from the excited state. (b) A snapshot of the electric-field components and populations at $t = 93$ ps superimposed on the micropillar refractive-index profile. (c) Zoom-in of the QD in (b) showing a snapshot of the level populations in the QD. (d) Time dynamics of the electric-field and level populations at the location of the QD. The population time evolution exhibits Rabi flopping at short times, and oscillations at longer times. (e) Zoom-in of (d) showing build-up of the final-state population, ρ_{33} ($\rho_{33max} \approx 0.04$). (f) Time evolution of the cavity emission exhibiting waveform reshaping.

ACKNOWLEDGMENTS

We acknowledge financial support for this work from the European Space Agency, ESA Contract No. 4000136394 /21/NL/GLC/ov: "Scalable cavity-embedded semiconductor quantum dot-based single-photon sources for QKD satellite quantum communication protocols."

REFERENCES

[1] Thomas, S. and Senellart, P., "The race for the ideal single-photon sources is on," *Nat. Nanotechnol.* **16**, 367–368 (2021).

[2] Knill, E., Laflamme, R., and Milburn, G. J., "A scheme for efficient quantum computation with linear optics," *Nature* **409**, 46 (2001).

[3] Cirac, J. I., Zoller, P., Kimble, H. J., and Mabuchi, H., "Quantum state transfer and entanglement distribution among distant nodes in a quantum network," *Phys. Rev. Lett.* **78**, 3221 (1997).

[4] Imamoğlu, A., Awschalom, D. D., Burkard, G., DiVincenzo, D. P., Loss, D., Sherwin, M., and Small, A., "Quantum information processing using quantum dot spins and cavity qed," *Phys. Rev. Lett.* **83**, 4204 (1999).

[5] Bergmann, K., Theurer, H., and Shore, B. W., "Coherent population transfer among quantum states of atoms and molecules," *Rev. Mod. Phys.* **70**, 1003–1025 (1998).

[6] Hennrich, M., Legero, T., Kuhn, A., and Rempe, G., "Vacuum-stimulated raman scattering based on adiabatic passage in a high-finesse optical cavity," *Phys. Rev. Lett.* **85**, 4872 (2000).

[7] Santori, C., Fattal, D., Fu, K.-M. C., Barclay, P. E., and Beausoleil, R. G., "On the indistinguishability of raman photons," *New J. Phys.* **11**, 123009 (2009).

[8] Kiraz, A., Atatüre, M., and Imamoğlu, A., "Quantum-dot single-photon sources: Prospects for applications in linear optics quantum-information processing," *Phys. Rev. A* **69**, 032305 (2004).

[9] Law, C. K. and Eberly, J. H., "Arbitrary controlof a quantum electromagnetic field," *Phys. Rev. Lett.* **76**, 1055–1058 (1996).

[10] Oreg, J., Hioe, F. T., and Eberly, J. H., "Adiabatic following in multilevel systems," *Phys. Rev. A* **29**, 690–697 (1984).

[11] Law, C. K. and Kimble, H. J., "Deterministic generation of a bit-stream of single-photon pulses," *J. Mod. Optics* **44**, 2067–2074 (1997).

[12] Marte, A. S. P. P., Zoller, P., and Kimble, H. J., "Synthesis of arbitrary quantum states via adiabatic transfer of zeeman coherence," *Phys. Rev. Lett.* **71**, 3095–3098 (1993).

[13] Kuhn, A. and Ljunggren, D., "Cavity-based single-photon sources," *Contemporary Physics* **51**, 289–313 (2010).

[14] Kuhn, A., Hennrich, M., Bondo, T., and Rempe, G., "Synthesis of arbitrary quantum states via adiabatic transfer of zeeman coherence," *Appl. Phys. B* **69**, 337–377 (1999).

[15] Sweeney, T. M., Carter, S. G., Bracker, A. S., Kim, M., Kim, C. S., Yang, L., Vora, P. M., Brereton, P. G., Cleveland, E. R., and Gammon, D., "Cavity-stimulated raman emission from a single quantum dot spin," *Nat. Photonics* **8**, 442–447 (2014).

[16] Pursley, B. C., Carter, S. G., Yakes, M. K., Bracker, A. S., and Gammon, D., "Picosecond pulse shaping of single photons using quantum dots," *Nat. Communications* **9**, 115 (2018).

[17] Cohen-Tannoudji, C., Dupont-Roc, J., and Grynberg, G., [*Atom-photon interactions*], Wiley-VCH Verlag GmbH & Co. KGaA (1998).

[18] Fleischhauer, M. and Manka, A. S., "Propagation of laser pulses and coherent population transfer in dissipative three-level systems: An adiabatic dressed-state picture," *Phys. Rev. A* **54**, 794–803 (1996).

[19] Poem, E., Kodriano, Y., Tradonsky, C., Lindner, N. H., Gerardot, B. D., Petroff, P. M., and Gershoni, D., "Accessing the dark exciton with light," *Nature Phys.* **6**, 993–997 (2010).

[20] Schwartz, I., Cogan, D., Schmidgall, E. R., Don, Y., Gantz, L., Kenneth, O., Lindner, N. H., and Gershoni, D., "Deterministic generation of a cluster of entangled photons," *Science* **354**, 434–437 (2016).

[21] Heindel, T., Thoma, A., Schwartz, I., Schmidgall, E. R., Gantz, L., Cogan, D., Strauß, M., Schnauber, P., Gschrey, M., Schulze, J.-H., Strittmatter, A., Rodt, S., Gershoni, D., and Reitzenstein, S., "Accessing the dark exciton spin in deterministic quantum-dot microlenses," *APL Photonics* **2**, 121303 (2017).

[22] Slavcheva, G., Koleva, M., and Rastelli, A., "Ultrafast pulse phase shift in a charged quantum dot- micropillar system," *Phys. Rev. B* **99**, 115433 (2019).

[23] Slavcheva, G. and Koleva, M., "Handbook of optoelectronic device modelling an simulation," **II, chap.IX**, 661–729, Taylor & Francis, CRC press, Boca Raton (2017).

[24] Slavcheva, G., "Model for the coherent optical manipulation of a single spin state in a charged quantum dot," *Phys. Rev. B* **77**, 115347 (2008).

[25] Gaubatz, J. R. K. U., Hioe, F. T., and Bergmann, K., "Adiabatic population transfer in a three-level system driven by delayed laser pulses," *Phys. Rev. A* **40**, 6741–6744 (1989).